Mol Neurobiol (2016) 53:4685–4700
DOI 10.1007/s12035-015-9396-7

Colistin-Induced Apoptosis of Neuroblastoma-2a Cells Involves the Generation of Reactive Oxygen Species, Mitochondrial Dysfunction, and Autophagy

Chongshan Dai[1] · **Shusheng Tang**[1] · **Tony Velkov**[2] · **Xilong Xiao**[1]

Received: 2 April 2015 / Accepted: 11 August 2015 / Published online: 28 August 2015

Abstract Neurotoxicity remains a poorly characterized adverse effect associated with colistin therapy. The aim of the present study was to investigate the mechanism of colistin-induced neurotoxicity using the mouse neuroblastoma2a (N2a) cell line. Colistin treatment (0–200 μM) of N2a neuronal cells induced apoptotic cell death in a dose-dependent manner. Colistin-induced neurotoxicity was associated with a significant increase of reactive oxygen species (ROS) levels, with a concomitant decrease in the activities of superoxide dismutase (SOD), catalase (CAT), and the glutathione (GSH) levels. Mitochondrial dysfunction was evident from the dissipation of membrane potential and the increase of Bax/Bcl-2, followed by the release of cytochrome c (CytC). Caspase-3/7, -8, and -9 activations were also detected. Colistin-induced neurotoxicity significantly increased the gene expression of p53 (1.6-fold), Bax (3.3-fold), and caspase-8 (2.2-fold) (all $p<0.01$). The formation of autophagic vacuoles was evident with the significant increases (all $p<0.05$ or 0.01) of both of Beclin 1 and LC3B following colistin treatment (50–200 μM). Furthermore, inhibition of autophagy by pretreatment with chloroquine diphosphate (CQ) enhanced colistin-induced apoptosis via caspase activation, which could be attenuated by co-treatment with the pan-caspase inhibitor Z-VAD-FMK. In summary, our study reveals that colistin-induced neuronal cell death involves ROS-mediated oxidative stress and mitochondrial dysfunction, followed by caspase-dependent apoptosis and autophagy. A knowledge base of the neuronal signaling pathways involved in colistin-induced neurotoxicity will greatly facilitate the discovery of neuroprotective agents for use in combination with colistin to prevent this undesirable side effect.

Keywords Colistin · Neurotoxicity · Oxidative stress · Apoptosis · Autophagy

Introduction

The dry antibiotic pipeline coupled to the spread of multidrug-resistant (MDR) pathogens has created a "perfect storm" where antibiotics are fast becoming useless [1]. The world is now facing a growing threat from the emergence of bacteria that are resistant to almost all available antibiotics [2]. Polymyxins (colistin and polymyxin B) are last-line lipopeptide antibiotics that are increasingly being used to treat life-threatening infections caused by MDR gram-negative bacteria [2–4]. Unfortunately, polymyxin therapy is thwarted by dose-limiting nephrotoxicity, which has been reported in up to 60 % of patients [5]. Neurotoxicity is another unwanted, albeit less common side effect [6, 7]. Patients receiving intravenous colistin methanesulfonate (CMS) (the inactive pro-drug of colistin [4]) therapy were reported to present with neurological symptoms such as confusion, dizziness, facial and peripheral paraesthesia, vertigo, seizures, respiratory muscle weakness, apnoea, and ataxia [6–9]. To date, the underlying mechanisms

Dr. Xilong Xiao is the first corresponding author and Dr. Tony Velkov is the co-corresponding author.

✉ Tony Velkov
tony.velkov@monash.edu

✉ Xilong Xiao
xiaoxl@cau.edu.cn

[1] College of Veterinary Medicine, China Agricultural University, 2 Yuanmingyuan West Road, Beijing 100193, People's Republic of China

[2] Drug Delivery, Disposition and Dynamics, Monash Institute of Pharmaceutical Sciences, Monash University, 381 Royal Parade, Parkville, Victoria 3052, Australia

of these neuropathic adverse effects remain poorly characterized. The development of a comprehensive cellular-level understanding the pathways involved in polymyxin-induced neurotoxicity is imperative if we are to improve the therapeutic index of these important last-line antibiotics. In the present study, we investigated the pathways of colistin-induced neurotoxicity using the N2a mouse neuroblastoma cell line. Our results demonstrate that colistin-induced neurotoxicity is strongly dose-dependent and involves both apoptotic and autophagy pathways. The significant potential of these pathways as neuroprotective targets is discussed.

Materials and Methods

Materials

Colistin (sulfate) was purchased from Zhejiang Shenghua Biology Co., Ltd (20 400 U/mg, Zhengjiang, China). Dulbecco's modified Eagle's medium (DMEM) and fetal bovine serum (FBS) were obtained from Life Technologies Corporation (Grand Island, NY, USA). 3-(4,5-Dimetylthiazol-2-yl)-2, 5-diphenyltetrazolium bromide (MTT), sodium dodecylsulfonate (SDS), and dimethyl sulfoxide (DMSO) were purchased from AMRESCO Inc. (Solon, OH, USA). Epotoside (purity ≥98 %), chloroquine diphosphate (CQ), sodium pyruvate, and phenylmethyl sulfonylfluoride (PMSF) were purchased from Sigma-Aldrich (St. Louis, MO, USA). Staurosporine (purity ≥98 %), Z-VAD-FMK (a pan-caspase inhibitor), *N*-acetylcysteine (NAC), bovine serum albumin (BSA), rhodamine (Rh) 123, and 2′,7′-dichlorofluorescensin diacetate (DCFH-DA) were purchased from Beyotime (Haimen, China). All other reagents were of analytical grade.

Measurement of Colistin-Induced Cytotoxicity

The N2a mouse neuroblastoma cell line (ATCC CCL-131™) was employed throughout in this study. N2a cells were cultured in DMEM medium supplemented with 10 % (*v*/*v*) FBS, 110 mg/L sodium pyruvate, 100 U/mL penicillin, and 100 μg/mL streptomycin (Beyotime, Haimen, China) at 37 °C in 5 % CO_2. The media were changed once per day. Cytotoxicity was measured by the MTT assay [10]; in brief, N2a cells (5×10^4) were seeded into 96-well tissue culture plates and incubated under the aforementioned conditions. After culture for 24 h, the cells were treated with 0–400 μM of colistin for 24 h. The medium was removed, and cells were incubated in 100 μL fresh medium containing 10 μL MTT solution (5 mg/mL in PBS) for 4 h at 37 °C. The medium was removed and replaced by 100 μL DMSO for 30 min. The MTT absorbance was measured at 570 nm using a microplate reader (Molecular Devices, Sunnyvale, CA, USA).

Colistin-induced damage to the plasma membrane of N2a cells was quantified by the amount of lactate dehydrogenase (LDH) released using a LDH assay kit (Beyotime, Haimen, China). The N2a cells were plated at a density of 5×10^5 cells/well in 12-well plates, cultured for 24 h, and then treated with colistin (0–400 μM) for 24 h. Then, the culture medium was harvested and centrifuged at 4000×*g* for 10 min at 4 °C. The LDH activity in the supernatant was measured by monitoring the absorbance at 490 nm. As a positive control, N2a neuronal cells were treated with etoposide at the final concentrations of 25 and 100 μM and staurosporine 10, 25, and 50 nM for 24 h.

Measurement of Intracellular ROS Generation

The production of intracellular ROS was measured using the ROS-specific fluorescent dye 2,7-dichlorofluorescein diacetate (DCFH-DA) (Beyotime, Haimen, China). N2a cells were seeded at an initial density of 2×10^4 cells/mL in 96-well plates. After 24 h, the medium were discarded and replaced with 200 μL DMEM containing colistin at final concentrations of 12.5, 25, 50, 100, and 200 μM and incubated at 37 °C for 24 h. The cells were then washed with PBS, followed by the addition of 200 μL DMEM containing 10 μM DCFH-DA and incubated for 30 min at 37 °C in the dark. After three washes with PBS, the DCFH-DA fluorescence was measured (excitation wavelength 488 nm, emission wavelength 530 nm). For further analysis of the role of oxidative stress in colistin-induced cytotoxicity, cells were pretreated for 1.5 h with NAC at 2.5 or 5 mM were before treatment with colistin at 200 μM.

Measurement of Intracellular Superoxide Dismutase, Catalase, and Glutathione

The SOD, CAT activity, and GSH content were measured using specific assay kits according to the manufacturer's instructions (Nanjing Jiancheng Co., Ltd., Nanjing, China). Briefly, cells were plated into 6-well plates at a density of 5×10^5 cells per well and treated with colistin at final concentrations of 0, 12.5, 25, 50, 100, and 200 μM at 37 °C for 24 h. The cells were washed with ice-cold PBS and lysed using the cell lysis buffer provided by the manufacturer. The cell lysates were centrifuged at 14,000×*g* for 10 min at 4 °C. The supernatants were collected and assayed for SOD, CAT activities, and GSH content. Protein concentrations were measured using a BCA™ protein assay kit (Beyotime, Haimen, China).

Measurement of Mitochondrial Membrane Potential

The inner membrane electrical potential across the mitochondrial membrane was measured as per our previously published methods [11]. Briefly, after colistin treatment at final concentrations of 0, 25, 50, 100, and 200 μM at 37 °C for 24 h. Epotoside (25 μM) and staurosporine (10 nM) were used as positive controls. The cells were washed with PBS and

harvested and then incubated with 0.5 μg/mL Rh123 dye in PBS for 30 min in the dark at 37 °C. The cells were washed twice with PBS and collected for determination of Rh123 fluorescence using a BD FACSAria™ flow cytometer (Becton Dickinson, San Jose, CA, USA).

Measurement of Caspase-3/7 and Caspase-9 Activities

N2a cells (1.5×10^4 cells per well) were cultured in 96-well plates and treated with colistin at final concentrations of 0, 25, 50, 100, and 200 μM at 37 °C for 24 h. Epotoside (25 μM) and staurosporine (10 nM) were used as a positive controls. The caspase-3/7 and -9 activities were determined using the Caspase-Glo® 3/7 and 9 assay kits (Promega Corp., Madison, USA) according to the manufacturer's instructions. The luminescence was measured using a microplate luminometer (Molecular Devices, Sunnyvale, CA, USA) and linearly related to the caspase-3/7, -8, and -9 activities.

To examine the effect of an inhibitor of autophagy (CQ) and apoptosis (Z-VAD-FMK), cells were pretreated with either CQ (10 μM) or Z-VAD-FMK (50 μM) per se or in combination (CQ, 10 μM + Z-VAD-FMK, 50 μM) for 1 h before treatment with colistin (200 μM). After 24 h, the caspase-3/7 activity was determined using the Caspase-Glo® 3/7 assay kits according to the manufacturer's instructions.

Flow Cytometric Analysis and Hoechst 33342 Staining of Apoptosis

N2a cells were cultured on 6-well plates at a density of 5×10^5 cells per well and treated with colistin at final concentrations of 0, 25, 50, 100, and 200 μM at 37 °C for 24 h. Epotoside (25 and 100 μM) and staurosporine (10 and 50 nM) were used as a positive controls. Flow cytometric analysis of apoptosis in N2a cells were carried out using an annexin V-FITC apoptosis detection kit (Vazyme Biotech Co., Ltd., Nanjing, China). In brief, colistin-treated cells were harvested with 0.25 % trypsin, washed twice with cold PBS, and resuspended in 500 μL binding buffer supplied by the manufacturer. The cells were then incubated with 5 μL annexin V-FITC (40 μg/mL) and 5 μL propidium iodide (40 μg/mL) in the dark for 10 min at room temperature and detected by BD FACSAria™ flow cytometry.

For Hoechst 33342 staining, N2a cells (2×10^5 cells per well) were cultured on 12-well culture plates and and treated with colistin at final concentrations of 0, 25, 50, 100, and 200 μM at 37 °C for 24 h. Epotoside (25 and 100 μM) and staurosporine (10, 25, and 50 nM) were used as positive controls. After staining with 1 μg/mL Hoechst 33342 (Vigorous Biotechnology, Beijing, China) for 20 min in the dark, the cells were observed under a fluorescence microscope (exCitation wavelength at 340 nm and emission wavelength at 510 nm) (Leica Microsystems, Wetzlar, Germany). Cells showing DNA fragmentation or chromatin condensation were counted as apoptotic cells.

Visualization of Monodansylcandaverine-labeled vacuoles

MDC is a fluorescent dye that is widely used as a specific marker for autophagic vacuoles [12]. N2a cells were seeded on to 12-well culture plates at a density of 2×10^5 cells per well and treated with colistin at final concentrations of 0, 25, 50, 100, and 200 μM at 37 °C for 24 h. Epotoside (25 μM) and staurosporine (10 nM) were used as positive controls. Cells were incubated with medium containing 5 μM MDC for 30 min in the dark at 37 °C. Finally, cells were washed twice with PBS and observed for MDC fluorescence using a fluorescence microscope (excitation wavelength 380 nm; emission wavelength 525 nm).

Microscopic Examination of Co-Staining of LC3 and Activated Caspase-3

Microscopic examination of co-staining of LC3 and activated caspase-3 were performed according to a previous study [13]. Briefly, N2a cells were seeded on to 12-well culture plates at a density of 2×10^5 cells per well and treated with colistin at final concentrations of 50 and 200 μM for 24 h and then were fixed with 4 % paraformaldehyde at room temperature for 30 min. The cells were then washed twice with PBS and then permeabilized with 1 % Triton X-100. The cells were next treated with blocking buffer (2 % bovine serum albumin in PBS) for 2 h. Cells were co-incubated with mouse LC3 antibodies (1:80; ProteinTech Group, Inc., Chicago, IL, USA) and activated caspase-3 (1:100; ProteinTech Group, Inc., Chicago, IL, USA) overnight at 4 °C, washed twice with PBS, followed by co-incubation with Cy3-labeled goat anti-rabbit and FITC-labeled goat anti-mouse IgG secondary antibodies (Beyotime Institution of Biotechnology, Haimen, China) (both 1:1000) for 2 h at 37 °C. The cells were then washed twice with PBS and incubated with 4′, 6-diamidino-2-phenylindole (DAPI) nuclear stain for 5 min. The expressions of activated caspase-3 and LC3 were examined under a fluorescence microscope at 570 nm (green) and 488 nm (red) filters, respectively.

Quantitative Reverse-Transcription PCR Examination

N2a cells were seeded on to 6-well culture plates at a density of 5×10^5 cells/well and treated with colistin at final concentrations of 0, 25, 50, 100, and 200 μM at 37 °C for 24 h, harvested, and total RNA was isolated using the TRIzol extraction kit (Invitrogen Inc, Carlsbad, CA) according to the manufacturer's instructions. cDNA was synthesized from

2 μg of total RNA using the Prime Script RT-PCR kit (Takara, Dalian, China). The PCR primers used were according to the previous study [14], as the following: p53: forward, 5′-AGA GTC TAT AGG CCC ACC CC-3′, reverse, 5′-GCT CGA CGC TAG GAT CTG AC-3′; caspase-8: forward, 5′-CAC TAG AAA GGA GGA GAT GGA AAG-3′, reverse, 5′-CTA TCC TGT TCT CTT GGA GAG TCC-3′; Bax: forward, 5′-GCC AGC AAA CTG GTG CTC AA-3′; reverse, 5′-ATG TCC AGC CCA TGA TGG TTC-3′; β-actin: forward, 5′-CGG GAA ATC GTG CGT GAC-3′, reverse, 5′-CAG GAA GGA AGG CTG GAA GAG-3′. qRT-PCR were performed using a Chromo 4™ instrument (Bio-Rad, Hercules, CA). The cycling conditions used were as follows: 95 °C for 10 min; 40 cycles of 95 °C for 15 s, 60 °C for 1 min, and 72 °C for 40 s. All reactions were conducted in triplicate. The fold change in gene expression was calculated using $2^{-\Delta\Delta Ct}$ after normalizing to the expression level of β-actin.

Western Blotting Analysis

N2a cells were seeded on to 6-well culture plates at a density of 5×10^5 cells/well and treated with colistin at final concentrations of 0, 25, 50, 100, and 200 μM at 37 °C for 24 h. Epotoside (25 μM) and staurosporine (10 nM) were used as positive controls. The cells were harvested using a scraper and lysed using 100 μL ice-cold lysis buffer (100 mM Tris–HCl, 2 % (*w*/*v*) SDS, 10 % (*v*/*v*) glycerol and pH 7.4; 1 mM PMSF, 1 μg/mL aprotinin, 1 μg/mL leupeptin, and 1 μg/mL pepstatin A). The lysates were then ultrasonicated (3 and 5 s apart in each cycle for 10 times, power 22 W) using an ultrasonic processor (Branson, Missouri, USA). Cell lysate samples were centrifuged at 14,000×*g* for 15 min at 4 °C, and supernatants were collected. The protein concentrations were measured using the BCA™ protein assay kit (Beyotime, Haimen, China). Western blotting was conducted as per our previously described methods with minor modifications to the original protocol [15]. The following primary antibodies were employed: rabbit polyclonal antibodies against Beclin 1 (1:2000; Santa Cruz Biotechnology), LC3B (1:1000), Bax (1:3000), Bcl-2 (1:1000), p62 (1:5000) (ProteinTech Group, Inc., Chicago, IL, USA); mouse monoclonal antibody against cytochrome C (CytC) (1:2000), GAPDH (1:1000), and β-actin (1:1000; Zhongshan Golden Bridge Co., Beijing, China). The secondary antibodies employed were goat anti-rabbit IgG (1:5000) or rabbit anti-mouse IgG (1:5000) (Zhongshan Golden Bridge Co., Beijing, China). The results were normalized to β-actin or GAPDH and analyzed using ImageJ (National Institute of Mental Health, Bethesda, MD, USA).

Statistical Analysis

All data are expressed as the mean ± standard deviation (SD) unless specified. Statistical analyses were conducted using SPSS V13.0 (SPSS Inc., Chicago, USA), and figures were prepared using Graph Pad Prism 5.0 (Graph Pad Software, Inc., La Jolla, CA). Unless otherwise specified, data from the control and treatment groups were analyzed with one-way analysis of variance (ANOVA), followed by the LSD post hoc test. A p value <0.05 was considered as significant.

Results

Colistin-Induced Neurotoxicity Is Dose-Dependent and Involves Apoptosis

The treatment of N2a neuronal cells with colistin for 24 h produced a significant dose-dependant decrease of cell viability ($p<0.05$ or 0.01, compared to the control) (Fig. 1a, b). The positive controls, epotoside, and staurosporine showed an expected decreases of cell viability (all $p<0.01$), in a dose-dependent manner. N2a cells exposed to colistin concentrations ≥50 μM also exhibited morphological changes such as cell body spindle-like, shrinkage, and dendrite fragmentation (Fig. 1c).

To gain further insights into the mode of cytotoxicity, cells were stained with Hoechst 33342 stain and quantitative analyzed by flow cytometry (Fig. 2a–d). Colistin-treated cells displayed more condensed and fragmented chromatin and bright blue nuclei, which are indicative of apoptosis (Fig. 2a). The positive control treatments with epotoside and staurosporine produced fragmentation of the nucleus into oligonucleosomes, in a dose-dependent manner (Fig. 2b). Furthermore, the early apoptotic and late apoptotic/necrosis stage ratios were investigated by flow cytometry. Following colistin treatment at final concentrations of 50, 100, and 200 μM, the early apoptotic cells increased to 14.2, 19.6, and 28.4 % (all $p<0.01$), respectively; whereas, the late apoptosis/necrosis stages increased to 9.7 % ($p<0.05$), 12.3 % ($p<0.01$), and 17.4 % ($p<0.01$), respectively (Fig. 2c). Compared with the positive controls, colistin at 200 μM that induced cell apoptotic death (early apoptotic cells + late apoptosis/necrosis) is approximately equal extent with epotoside at 100 μM (48.8 vs 44.7 %), was more than staurosporine at 10 nM (48.8 vs 27.3 %), but much lower than staurosporine at 50 nM (48.8 vs 83.9 %).

Colistin-Induced Neurotoxicity Involves ROS Production and Oxidative Stress

The treatment of N2a cells with colistin at final concentrations of 50, 100, and 200 μM for 24 h significantly increased the ROS levels to 124.8 ($p<0.05$), 157.8 % ($p<0.01$), and 204.5 % ($p<0.01$) (Fig. 3a). Concomitantly, the activities of CAT, SOD, and the GSH levels were significantly decreased (Fig. 3b–d). Notably, there was no significant change on

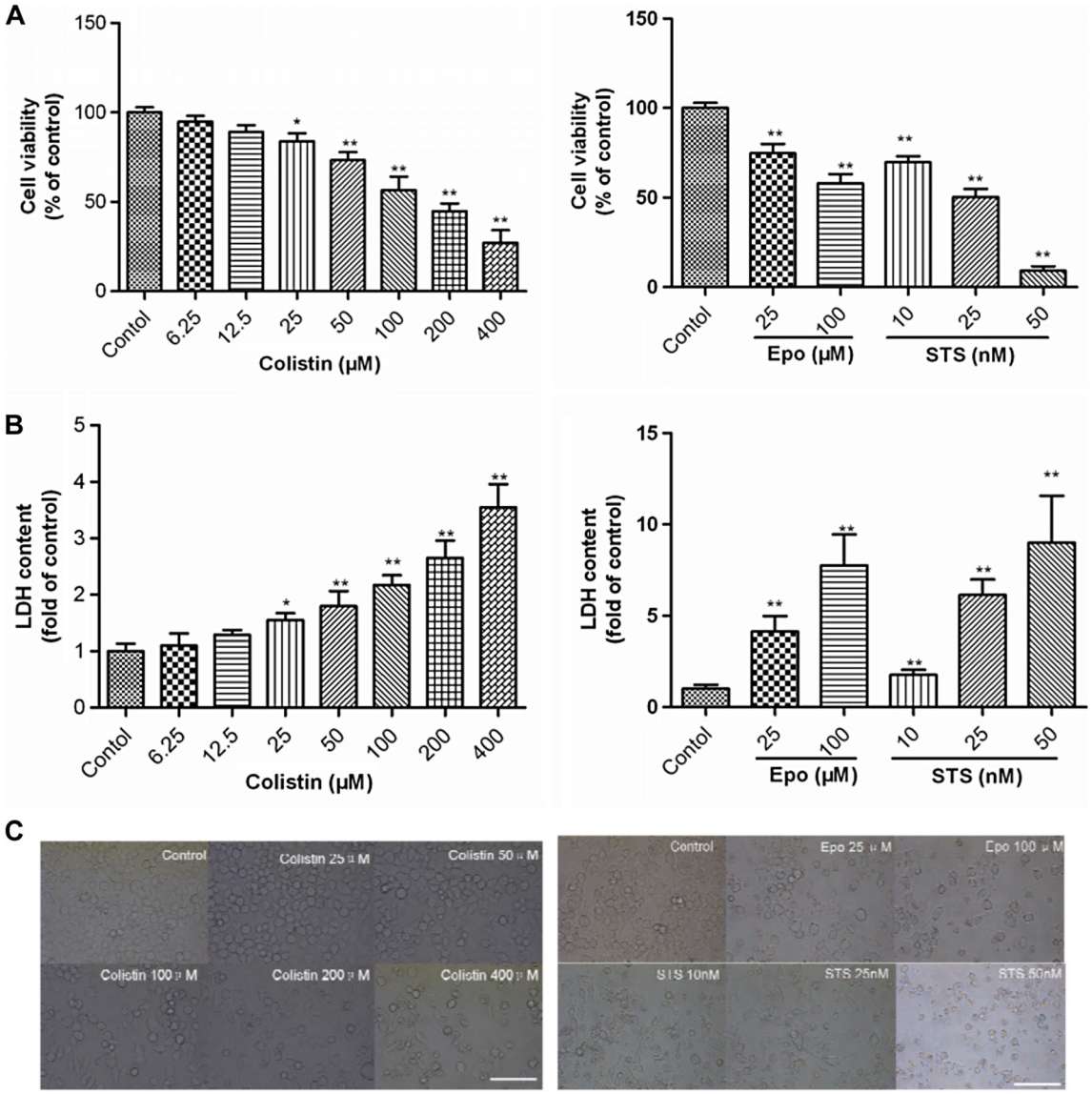

Fig. 1 Colistin-induced cytotoxicity of neuroblastoma N2a cells. **a** The changes in cell viability of N2a cell treated with colistin, etoposide, or staurosporine. **b** LDH release was determined following treatment with colistin (0 to 400 μM) for 24 h; etoposide and staurosporine were used as the positive control treatments. Values are presented as mean ± SD ($n=5$). *$p<0.05$, **$p<0.01$, compared to the control group. **c** Corresponding light microscope images of N2a cells treated with colistin (*scale bar*= 50 μm). *Epo* etoposide, *STS* staurosporine

intracellular ROS, SOD, CAT, and GSH levels when N2a cells were exposed to colistin at concentrations of ≤25 μM for 24 h (Fig. 3a–d).

Colistin-Induced Neurotoxicity Involves Mitochondrial Dysfunction and Caspase Activation

The treatment of N2a cells with colistin at final concentrations of 50, 100, and 200 μM for 24 h significantly decreased the mitochondrial membrane potential (MMP) to 86.7 % (colistin at 50 μM; $p<0.01$), 72.4 % (colistin at 100 μM; $p<0.01$), and 58.1 % (colistin at 200 μM; $p<0.01$), compared to that in control group. The positive control treatments etoposide (25 μM) and staurosporine (10 nM) significantly decreased MMP to 76.4 and 76.8 %, respectively (Fig. 4a). Colistin treatment concomitantly increased the release of CytC and the Bax/Bcl-2 ratio that also significantly increased in the positive control treatments ($p<0.01$) (Fig. 4b). Caspase-3/7, -8, and -9 activities were all significantly ($p<0.05$ or 0.01) increased following colistin treatment at concentrations ≥50 μM and were markedly increased when N2a cell were treated with etoposide at 25 μM and staurosporine 10 nM (Fig. 4c).

Moreover, pretreatment of the cells with NAC (2.5 and 5 μM), an inhibitor of oxidative stress, markedly reduced

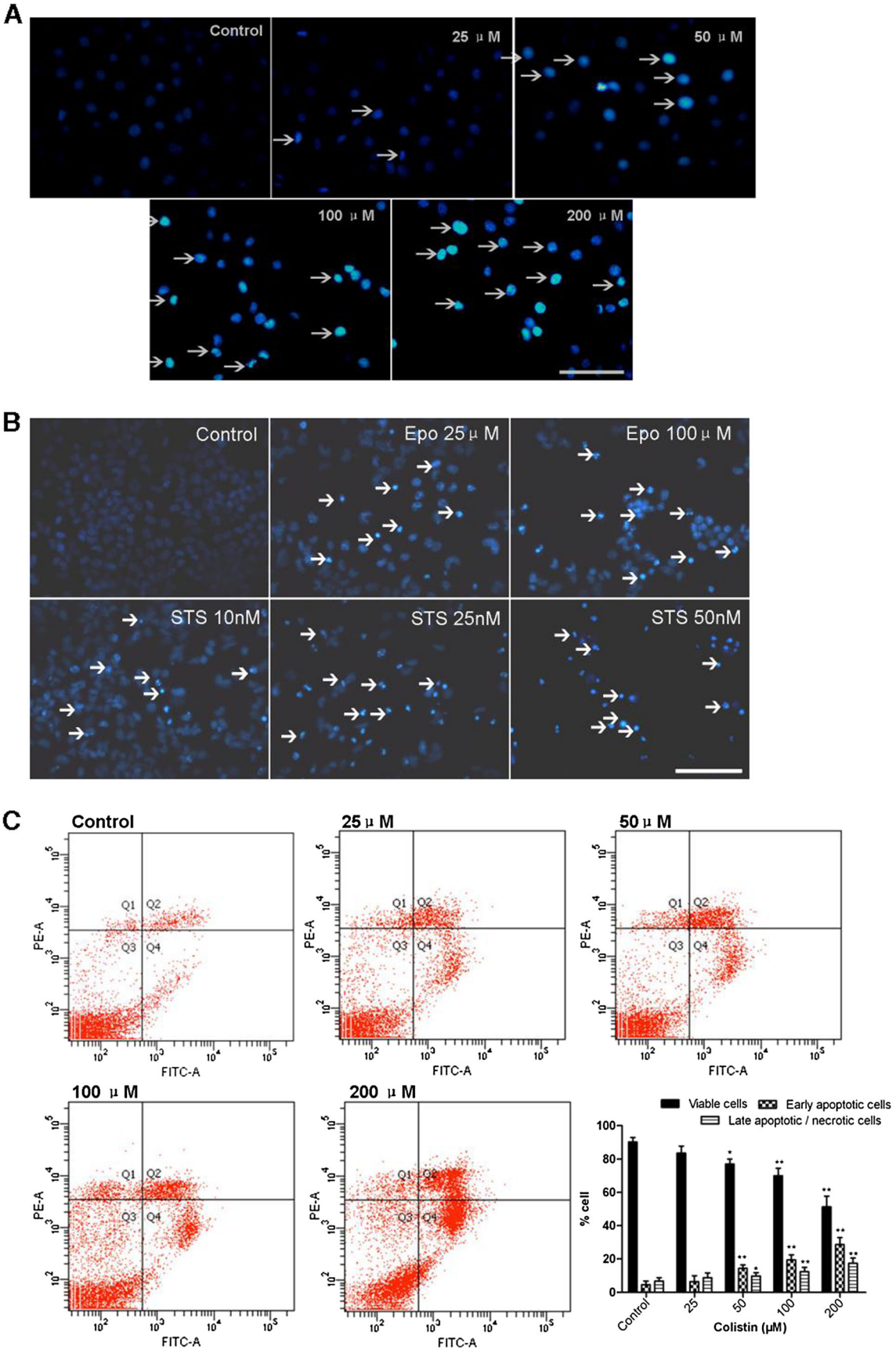
A
Control
25 μ M
50 μ M
100 μ M
200 μ M
B
Control
Epo 25 μ M
Epo 100 μ M
STS 10nM
STS 25nM
STS 50nM
C
Control
25 μ M
50 μ M
100 μ M
200 μ M
PE-A
FITC-A
Q1
Q2
Q3
Q4
Viable cells
Early apoptotic cells
Late apoptotic / necrotic cells
% cell
Colistin (μM)
Control
25
50
100
200

◀ **Fig. 2** Colistin-induced apoptosis in neuroblastoma N2a cells. **a** Colistin-induced fragmentation of the nucleus into oligonucleosomes and chromatin condensation were examined and photographed by fluorescence microscopy following Hoechst 33342 staining. The *white arrows* indicate apoptotic cells. *Scale bar*=50 μm. **b** Etoposide and staurosporine were used as the positive control treatments. The *white arrows* indicate apoptotic cells. *Scale bar*=25 μm. **c** Monitoring of colistin-induced cellular apoptosis by flow cytometry following annexin V-FITV/PI staining. **d** Monitoring of etoposide- or staurosporine-induced cellular apoptosis by flow cytometry following annexin V-FITV/PI staining. All values were presented as mean ± SD, from three independent experiments (n=3). *p<0.05, **p<0.01, compared to control group; *Q1* necrosis cells, *Q2* later apoptotic cells, *Q3* survival cells, *Q4* early apoptotic cells, *Epo* etoposide, *STS* staurosporine

the production of ROS, caspase-3 activity, and colistin-induced apoptosis (all p<0.01) (Fig. 5).

Colistin-Induced Neurotoxicity Upregulates the Expression of p53, Caspase-8, and Bax

Colistin treatment of N2a cells at the final concentrations of 25, 50, 100, and 200 μM for 24 h induced an upregulation of p53, caspase-8, and Bax gene expression (Fig. 6). Colistin treatment at concentration ≥25 μM significant increased the Bax messenger RNA (mRNA) levels (p<0.05 or 0.01) to 3.3-fold at 200 μM colistin. Similarly, a colistin concentration ≥50 μM treatment increased caspase-8 and p53 mRNA levels to 2.2- and 1.6-fold (colistin at 200 μM) (both p<0.01), respectively.

Colistin Neurotoxicity Activates Autophagy

Treatment of N2a cells with colistin at final concentrations of 25–200 μM for 24 significantly increased neuronal cell autophagy in a dose-dependent manner (Fig. 7). Western blotting revealed that the relative expression levels of Beclin 1 and the ratio of LC3II/I were significantly increased (~3.5-fold at colistin 50 μM); this was also evident with the positive control treatments with etoposide (25 μM) and staurosporine (10 nM) (Fig. 7a). The formation of acidic vesicular organelles (AVOs) was also evident following colistin (25–200 μM), etoposide (25 μM), and staurosporine (10 nM) treatment for 24 h (Fig. 7b, c). Figure 7d depicts immunofluorescence images that show the co-expression of LC3 and activated caspase-3 upon colistin treatment.

Inhibition of Autophagy Enhances Colistin-Induced Apoptosis and Caspase Activation

Figure 8a shows the marked increase of N2a cell death upon pretreatment with the autophagy inhibitor CQ. Moreover, we observed that CQ treatment increased the activation of caspase-3/7, p62, and LC3 expression and inhibition of Beclin 1 expression (Fig. 8b, c). Co-treatment of the cells with both the

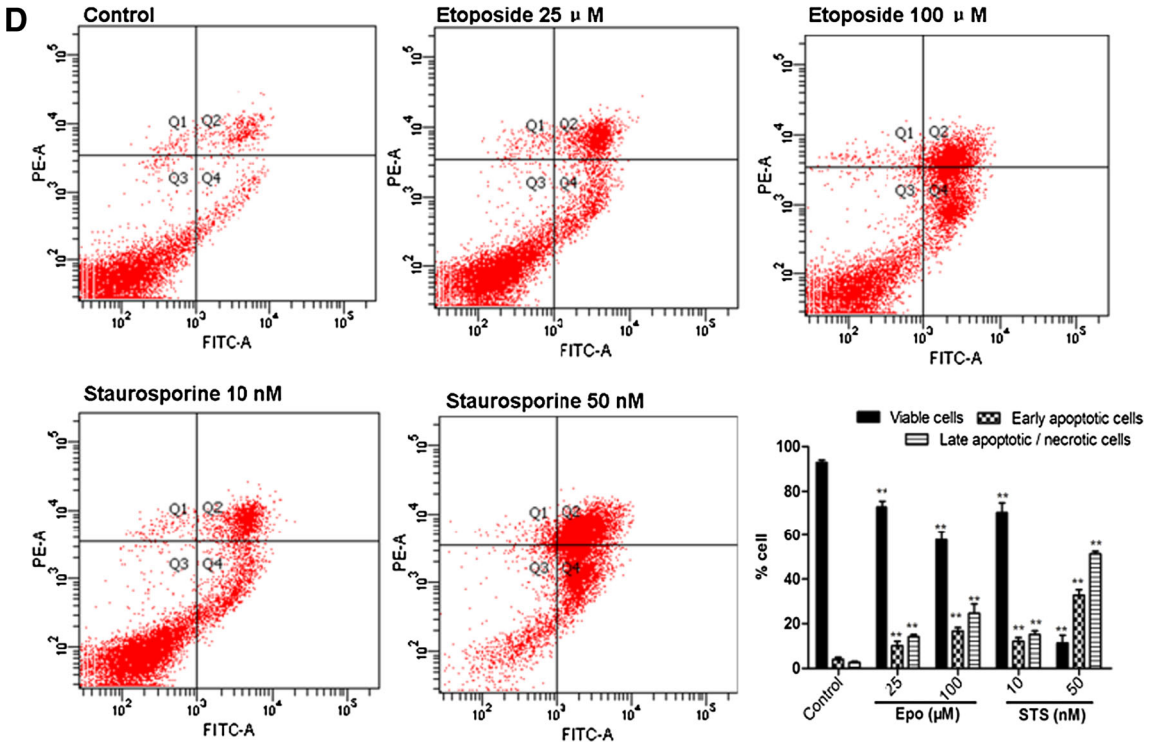

Fig. 2 (continued)

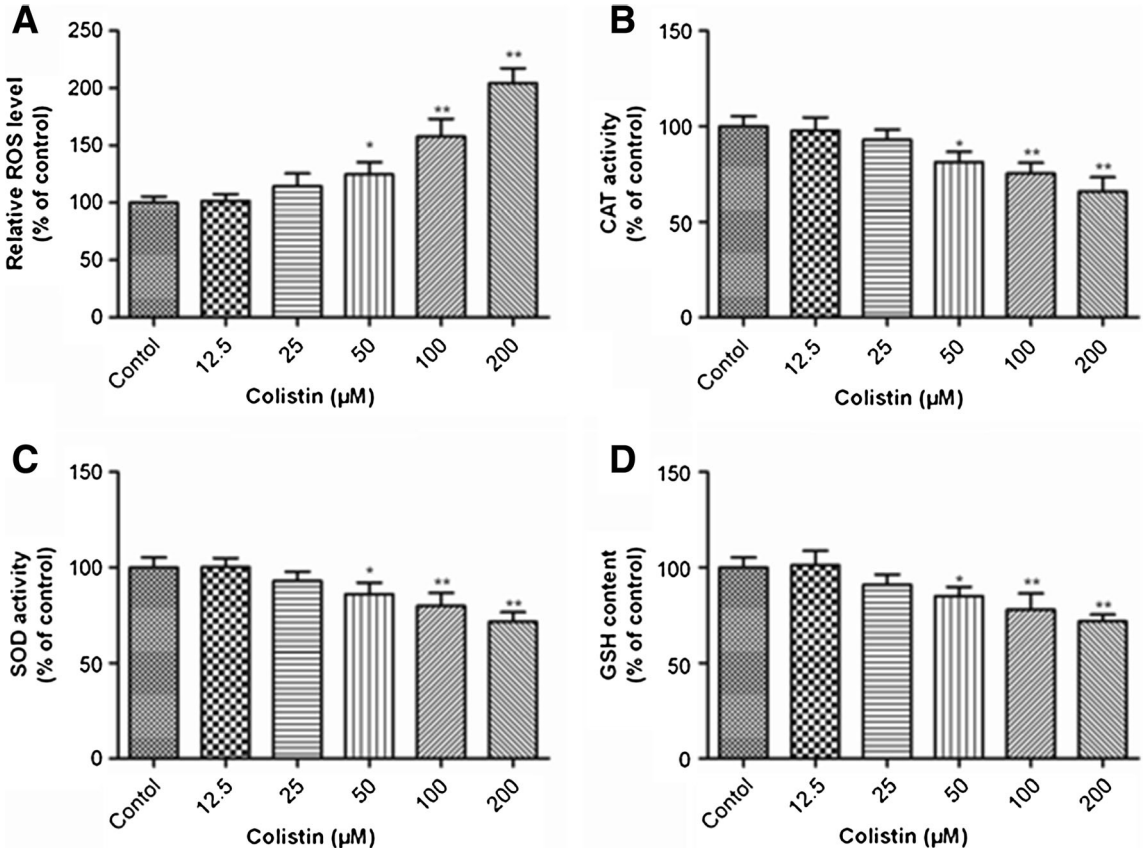

Fig. 3 Colistin-induced oxidative stress in neuroblastoma N2a cells. **a** ROS production in response to colistin treatment. Intracellular ROS production was measured fluorimetrically using the dye 2,7-dichlorofluorescein diacetate. **b**–**d** Impact of colistin treatment on cellular catalase (CAT), superoxide dismutase (SOD) activities, and glutathione (GSH) levels. Values are presented as the mean ± SD, from three independent experiments (n=3). *p<0.05, **p<0.01, compared to the control

autophagy inhibitor CQ and the pan-caspase inhibitor Z-VAD-FMK markedly attenuated all of these events (Fig. 8b, c).

Discussion

The polymyxins were discovered in the 1950s but never subjected to contemporary drug safety and development procedures [1, 7]. Neurotoxicity is the second major, albeit poorly understood side effect associated with polymyxin therapy [6, 7]. Clinical symptoms of polymyxin-induced neurotixicity include dizziness, visual disturbances, vertigo, confusion, hallucinations, seizures, ataxia, and facial and peripheral paresthesias. An early study of the safety of intramuscularly administered colistimethate sodium (CMS) indicated that 7.3 % of the patients developed neurotoxicity during the first 4 days of therapy [16]; symptoms of mild neurotoxicity (such as paresthesias) tend to be more frequent, especially in elderly patients, but are often ignored because of the lack of objective assessment protocols [6, 7, 17, 18]. Multiple animal studies have shown that colistin can induce neurotoxicity in mice [19, 20], rats [21], pigs [22], or ostriches [23]. Notably, our mouse model studies demonstrated that high doses (15 mg/kg/day for 3 or 7 days) of colistin administered intravenously can cause marked neurotoxicity and neuronal damage of the brain [17, 19]. In the present study, we employed the N2a mouse neuroblastoma cell line to investigate the molecular mechanisms underlying colistin-induced neurotoxicity.

In the present study, we demonstrated that colistin treatment for 24 h caused a decrease of cell viability and apoptosis in N2a cells in a dose-dependent manner (Figs. 1 and 2). These findings are consistent with our previous studies that demonstrated that colistin can induce apoptosis in primary chicken cortex neurons [24, 25]. These findings are not surprising given that it has been well established that apoptosis plays a critical role in maintaining brain homeostasis in response to drug-induced toxicity [26–28]. Our pathway mapping data indicate that colistin-induced apoptosis in neuronal cell is activated via both the death receptor (extrinsic) and the mitochondrial (intrinsic) pathways [29]. The activation of the mitochondrial pathway was clearly evident based on several key findings. Colistin treatment of neuronal cells induced a rapid dissipation of the mitochondrial membrane potential (Fig. 3a), indicative of mitochondrial dysfunction. The

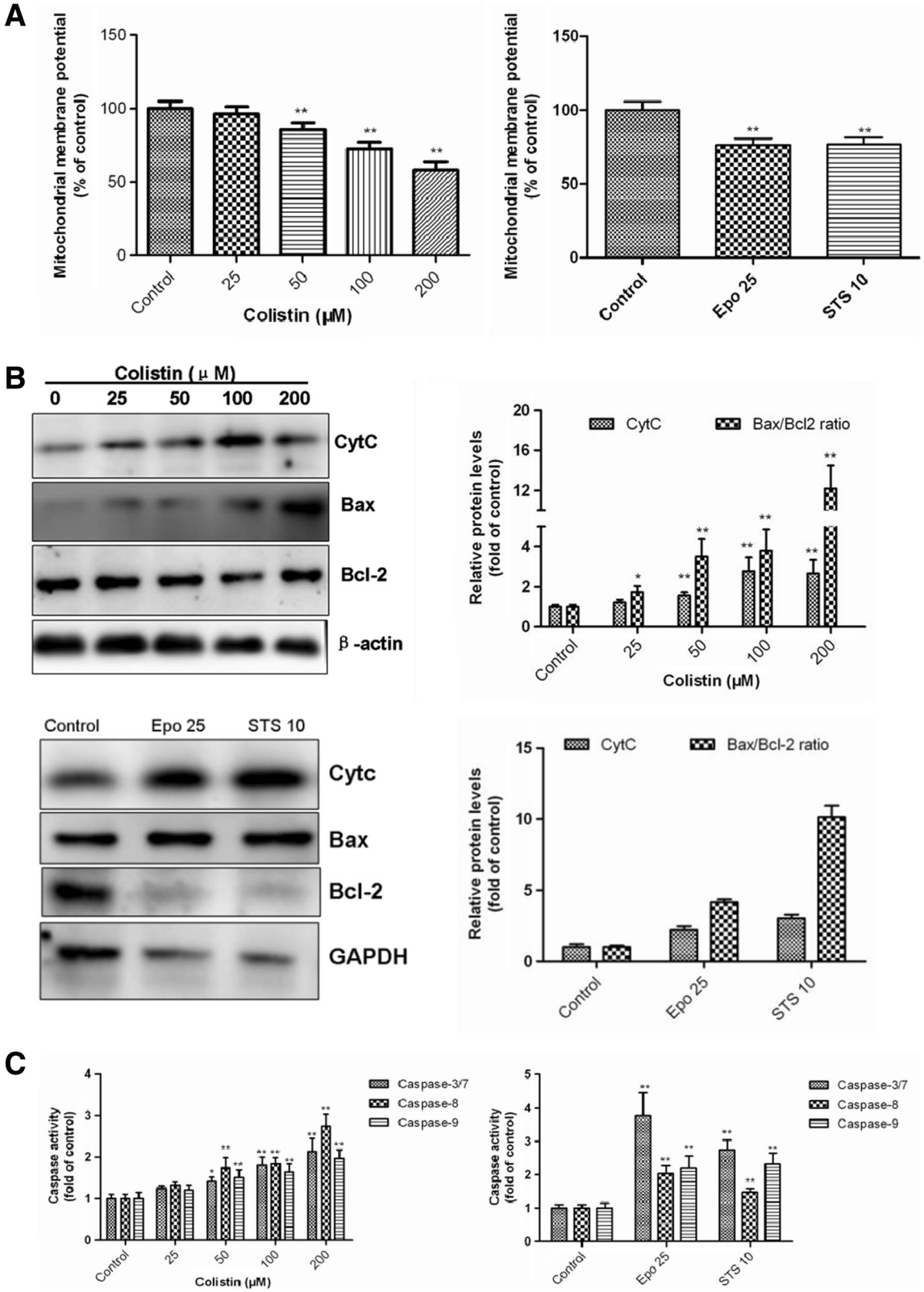

Fig. 4 Colistin-induced mitochondrial dysfunction and caspase activation apoptosis in neuroblastoma N2a cells. **a** Colistin-induced dissipation of mitochondrial membrane potential (Δψm); etoposide and staurosporine were used as the positive control treatments. **b** Colistin treatment increases the Bcl2/Bax ratio and cytochrome C (Cyt C) release; β-actin or GAPDH was used as the internal standard. **c** Activation of caspase-3/7, -8, and -9 in response to colistin treatment. Values were presented as mean ± SD, from three independent experiments ($n=3$). *$p<0.05$, **$p<0.01$, compared to the control. *Epo* etoposide, *STS* staurosporine

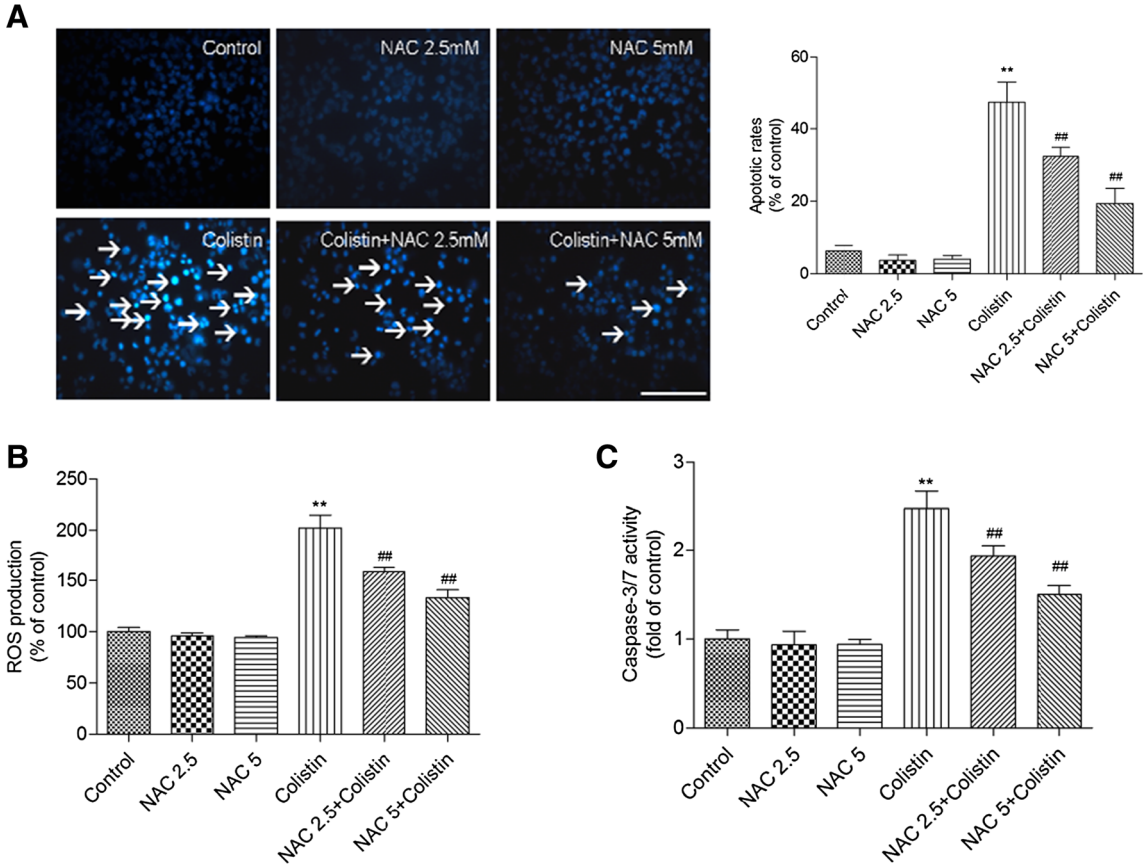

Fig. 5 Antioxidant NAC inhibits colistin-induced ROS production, caspase-3 activity, and apoptosis. N2a cells were pretreated with NAC at the final concentrations of 2.5 and 5 mM for 1.5 h before treatment with colistin (200 μM); **a** after 24 h, cellular apoptotic rates were examined and counted by using Hoechst 33342 staining. The *white arrows* indicate apoptotic cells. *Scale bar*=25 μm; **b**, **c** Changes of ROS production and caspase-3 activity, respectively. Values were presented as mean ± SD, from three independent experiments (n=3). *p<0.05, **p<0.01, compared to the control; $^{\#}p$<0.05, $^{\#\#}p$<0.01, compared to colistin alone

mitochondrial pathway is regulated by the pro- and anti-apoptotic Bcl-2 family proteins including Bax and Bcl-2 [30]. An increase in the Bax/Bcl-2 ratios and CytC release was evident upon colistin treatment (Fig. 4a); these events are concordant with mitochondrial outer membrane permeabilization [31]. The release of CytC into the cytoplasm leads to the activation of caspase-3 and -9 (Fig. 4c), which, in turn, trigger apoptosis. Our results showed that colistin treatment significantly increased caspase-8 (executor) activity and mRNA levels (Figs. 4c and 6). This would suggest that colistin-induced apoptotic neuronal cell death can also occur via the death receptor pathway. Notably, colistin treatment significantly increased the level of p53 mRNA (Fig. 6). p53 is involved in mediating cross talk between the mitochondrial and death receptor pathways by regulating caspase-8 gene expression and subsequently resulted in events concerned with mitochondrial dysfunction [15, 32–34]. p53 can also directly activate Bax which permeabilizes mitochondria, causing mitochondrial CytC release and caspase activation, which triggers apoptosis [35]. This is consistent with the ~3.3-fold increase in Bax mRNA levels we observed following treatment of the N2a cells with 200 μM colistin (Fig. 6).

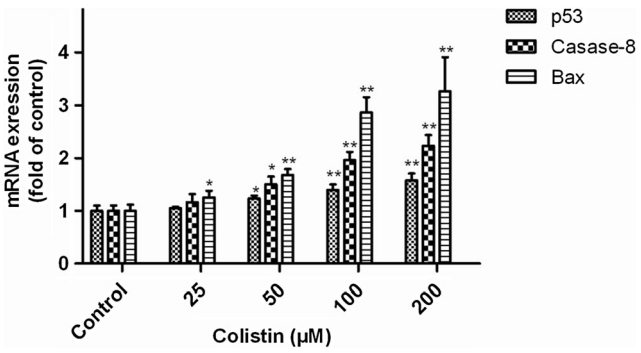

Fig. 6 Colistin treatment upregulates the mRNA expression levels of p53, caspase-8, and Bax in neuroblastoma N2a cells. All values are presented as the mean ± SD, from three independent experiments (n=3). *p<0.05, **p<0.01, compared to control group

The nervous system is particularly vulnerable to oxidative damage owing to its high utilization of oxygen, high content of polyunsaturated fatty acids, and relatively low antioxidant levels [36]. Mitochondria are a major source of ROS [37].

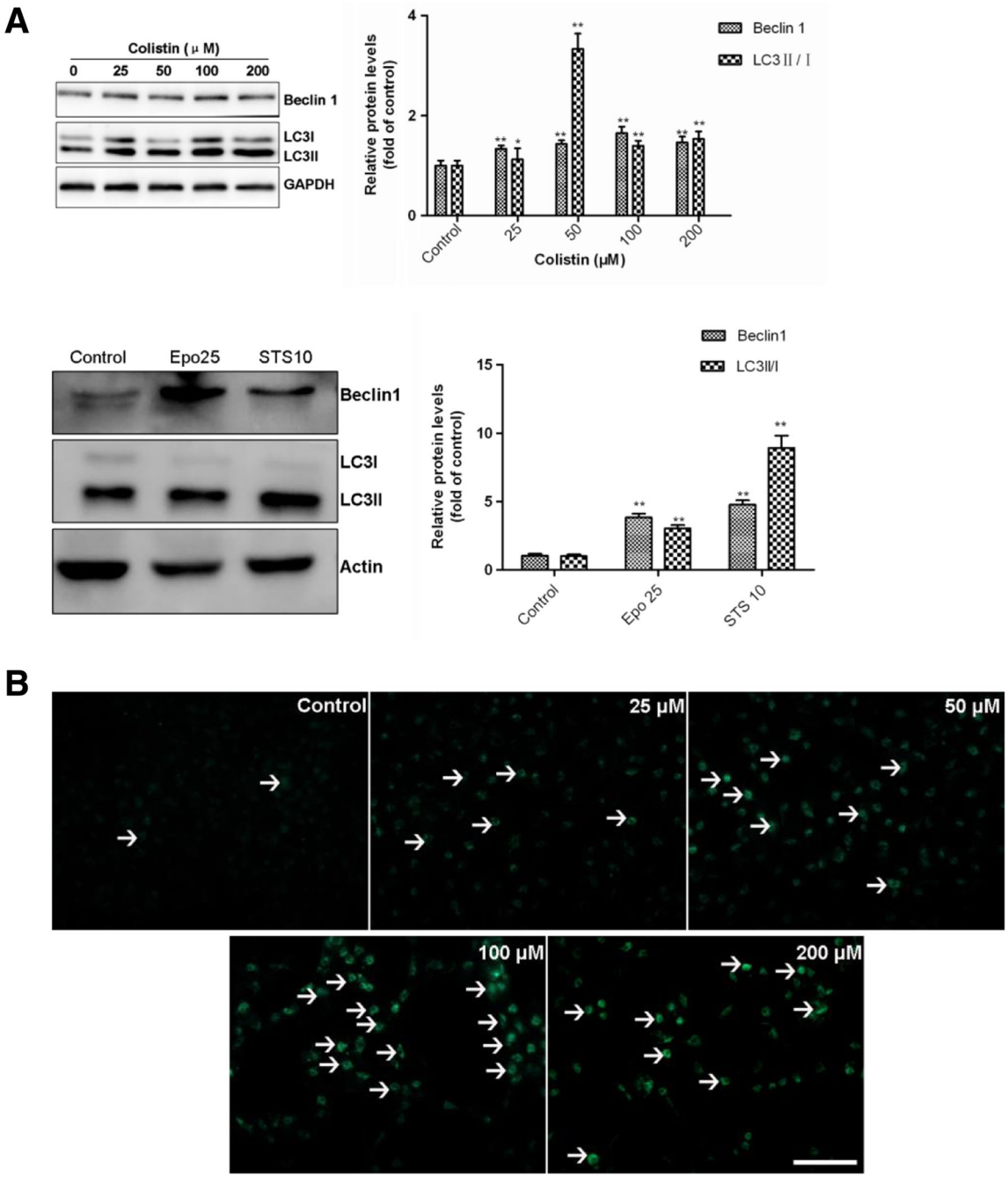

Fig. 7 Colistin treatment activates autophagy in neuroblastoma N2a cells. **a** The expression levels of Beclin 1 and the ratio of LC3II/I were determined by Western blotting following colistin treatment for 24 h. Etoposide and staurosporine were used as the positive controls. Values were presented as mean ± SD, from three independent experiments (n= 3). *p<0.05, **p<0.01, compared to the control. **b** Fluorescence imaging of colistin-treated cells following MDC staining (magnification ×20). *White arrows* indicate acidic vesicular organelles (AVOs). **c** Fluorescence imaging of etoposide at 25 μM (i.e., Epo 25) or staurosporine 10 nM (i.e., STS 10) treated cells following MDC staining (magnification ×20). *White arrows* indicate acidic vesicular organelles (AVOs) *Scale bar*=25 μm. **d** Co-immunofluorescence staining with LC3 (*green*) and activated caspase-3 (*red*) antibody, and the nuclear stain DAPI (*blue*). *Scale bar*=50 μm

Mitochondrial dysfunction is closely related to excessive ROS accumulation, which leads to damage to lipids, proteins, and DNA, ultimately resulting in cell death [38]. We previously detected mitochondrial dysfunction in the mouse cerebral cortex and sciatic nerve tissues in mice intravenously injected with 15 mg/kg/day colistin sulfate for 7 days [19, 20]. In the present study, we found that intracellular ROS levels in N2a cells significantly increased following colistin treatment (Fig. 3a). Concomitantly, we observed a decrease in GSH levels and in the activity of the antioxidant enzymes SOD

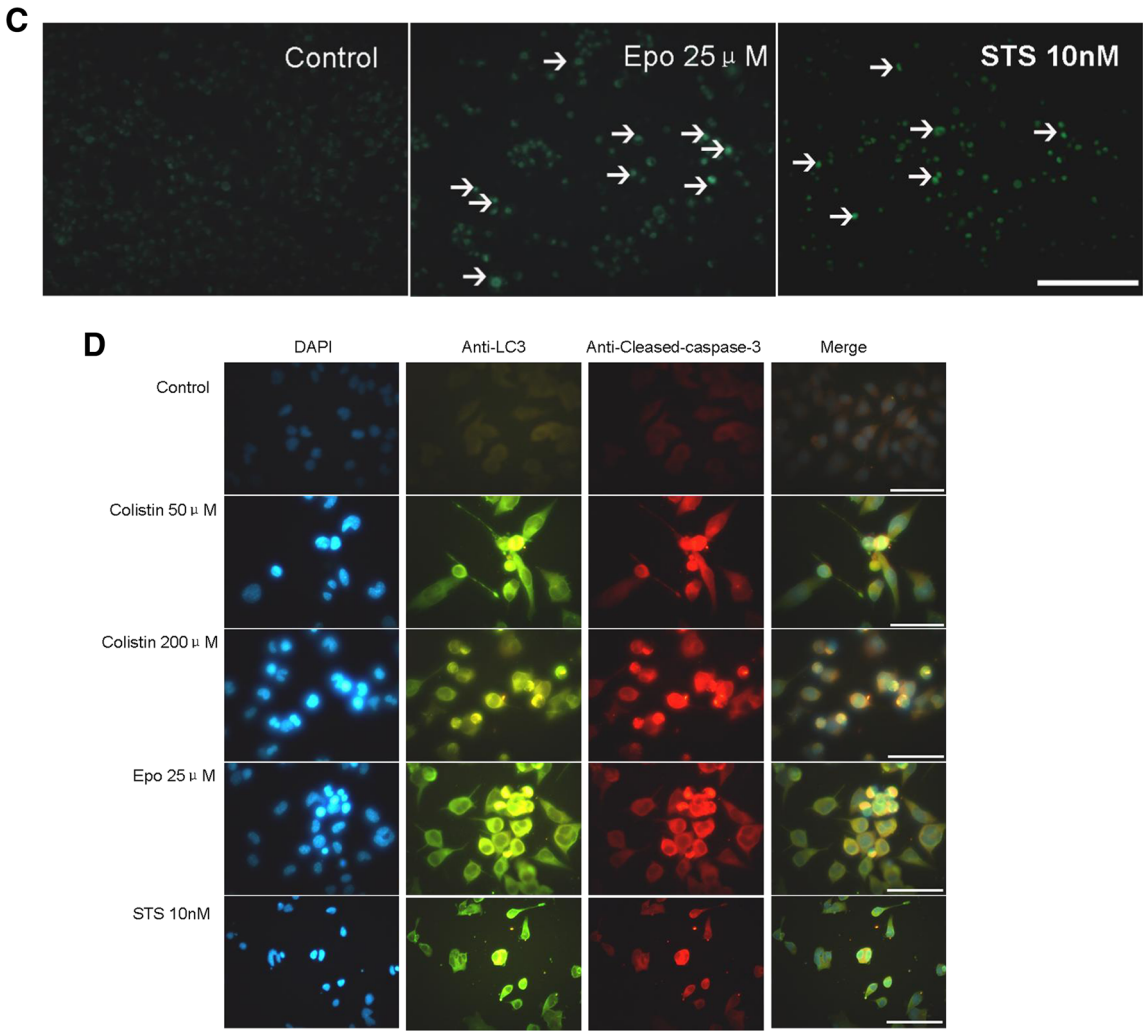

Fig. 7 (continued)

and CAT (Fig. 3b–d). This indicates that colistin exposure decreases a neurons' capacity to breakdown superoxide anions and hydroxyl radicals, further exacerbating ROS-mediated oxidative stress. Generation of ROS, secondly activation of the release of pro-apoptotic proteins from mitochondria or directly damage of DNA, can all trigger the activation of different modes of cell death, such as necrosis or apoptosis [14]. Furthermore, our results showed that pretreatment with the antioxidant NAC can effectively inhibit colistin-induced production of ROS, caspase activation, and apoptosis (Fig. 6). These findings demonstrate that there is potentially a direct relationship between oxidative stress and colistin-induced apoptosis. Coincidently, we have previously demonstrated that the co-administration of antioxidants such as lycopene is protective against polymyxin-induced nephrotoxicity in mice [39]. In our study demonstrated that ascorbic acid can markedly inhibit colistin-induced oxidative stress-mediated apoptosis in PC12 neuronal cell [10]. Taken together, these findings support the notion that oxidative stress pathways play an important role in polymyxin-induced neurotoxicity.

Autophagy and apoptosis control the turnover of organelles and proteins within cells and of cells within organisms, respectively [40]. Many stress including nutrient deprivation, hypoxia, oxidative stress, and DNA damage can sequentially elicit autophagy and apoptosis within the same cell [40]. In general, autophagy blocks the induction of apoptosis or delay apoptotic cell death, and apoptosis-associated caspase activation shuts off the autophagic process [37, 40]. For example, some studies have shown that co-treatment with autophagy inhibitors, such as CQ, or knockdown of autophagy genes, such as Beclin 1 and autophagy-related (Atg) genes, enhanced drug-induced apoptosis [41–43]. In the present study, we demonstrated that colistin-induced N2a cell death involves autophagy, as confirmed by the formation of autophagic vacuoles and the upregulation of the autophagy markers Beclin 1, p62, and LC3II/I (Figs. 7 and 8). Importantly, we observed an

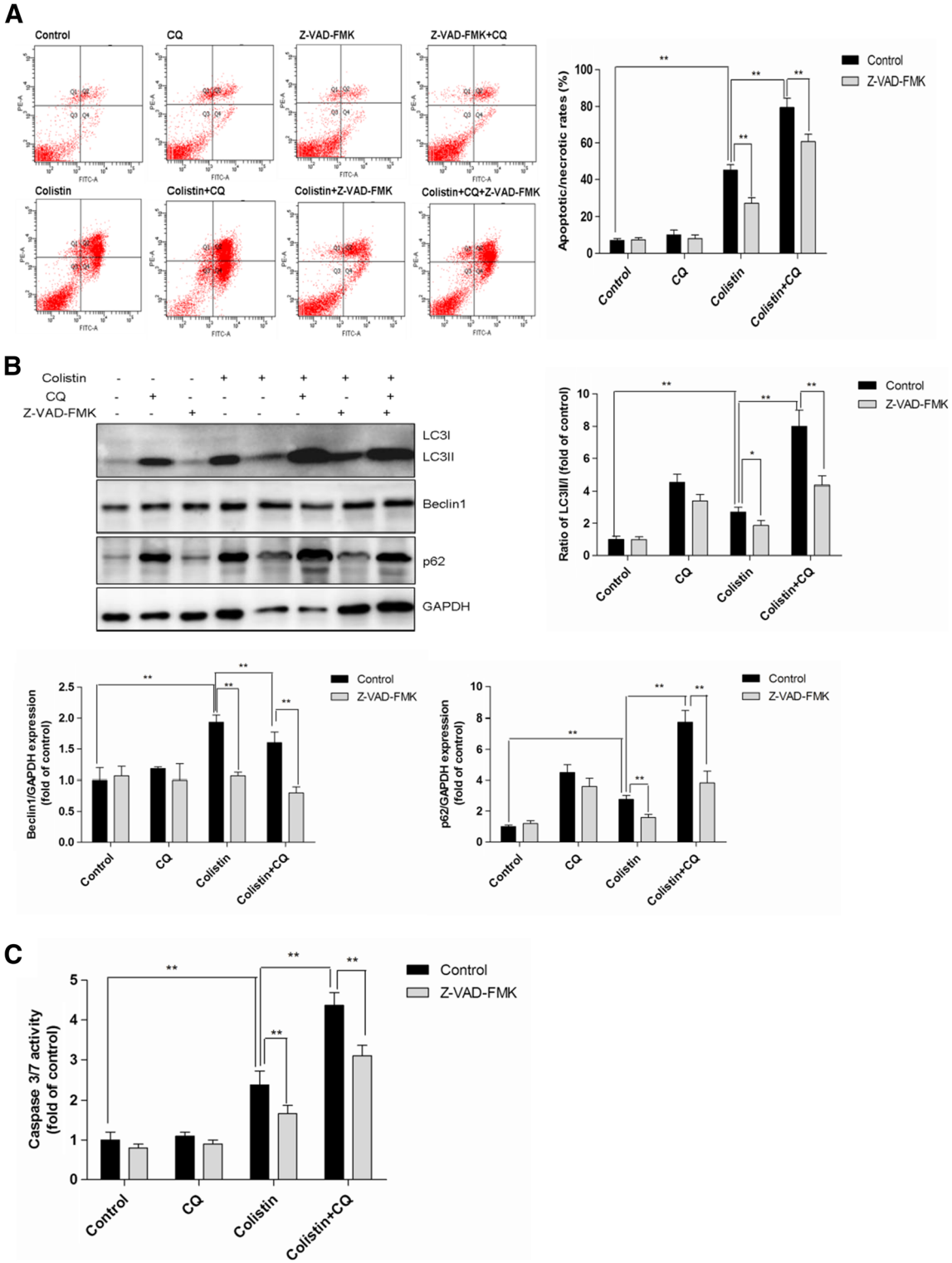

Fig. 8 Inhibition of autophagy enhances colistin-induced apoptosis and caspase activation in neuroblastoma N2a cells. N2a cells were pretreated with either the autophagy inhibitor CQ (10 μM) or the pan-caspase inhibitor Z-VAD-FMK (50 μM) per se or in combination (CQ, 10 μM + Z-VAD-FMK, 50 μM) for 1 h before treatment with colistin (200 μM). After 24 h, the cell apoptosis (**a**), markers of autophagy (**b**), and caspase-3/7 activity (**c**) were examined, respectively. Student's *t* test was used to compare results between the control and the samples. *$p<0.05$, **$p<0.01$

increase of N2a apoptotic cell death upon pretreatment with the late phase autophagy inhibitor CQ (which prevents lysosomal degradation [41]). This would suggest that autophagy inhibition synergizes with apoptosis to induced cell death.

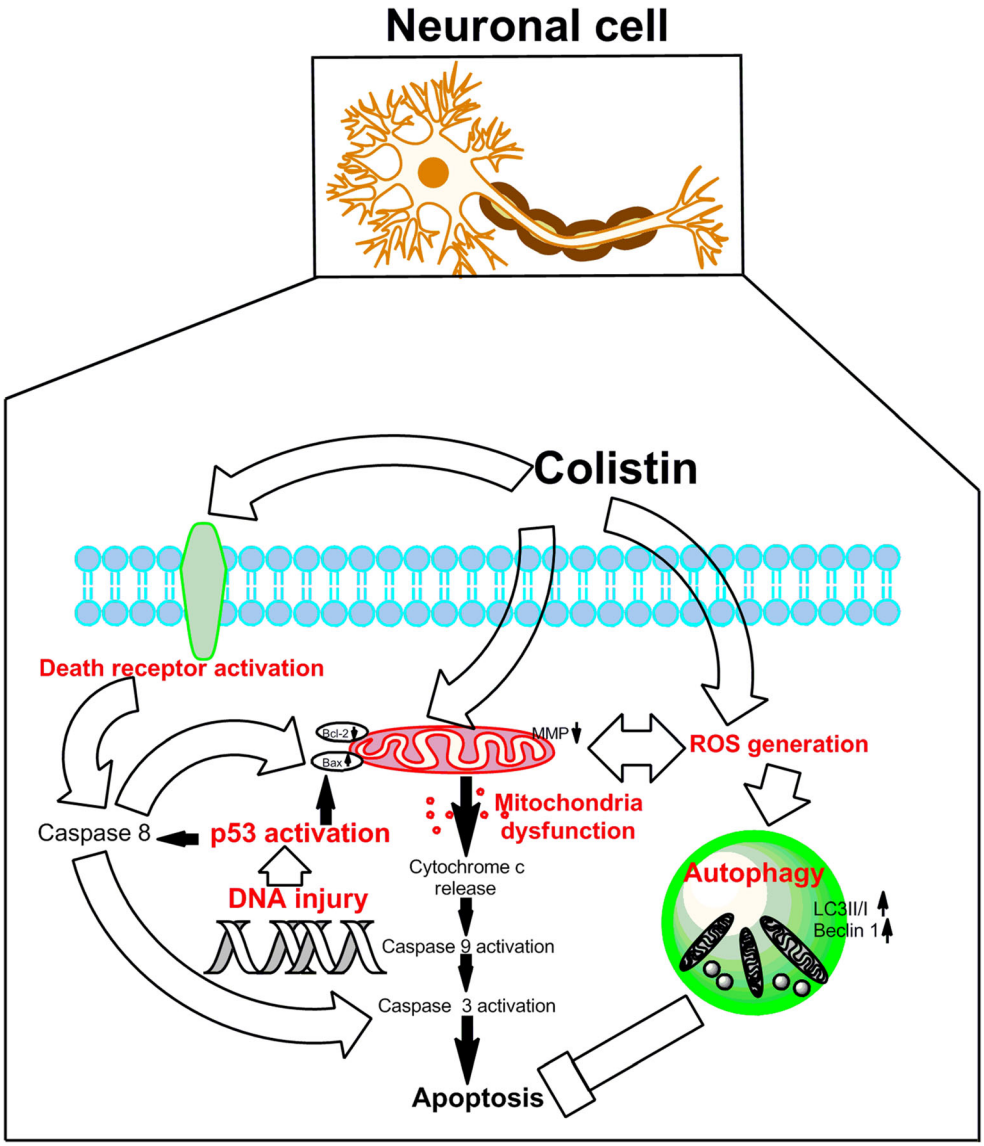

Fig. 9 A schematic representation of the apoptotic pathways involved in colistin-induced neuroblastoma N2a cell death. Colistin-induced apoptosis involves the activation of death receptor and mitochondrial pathways (aberration of the Bax/Bcl2 ratio, loss of membrane potential and production of reactive oxygen species [ROS]), activation of caspase-3, -8, and -9, and, finally, DNA fragmentation resulting in neuronal cell death. Autophagy may play a neuroprotective role

Since caspases play a critical role in mediating the complex cross talk between autophagy and apoptosis [44, 45], it is not surprising that all of these events were attenuated upon co-treatment of the N2a cells with both the autophagy inhibitor CQ and the pan-caspase inhibitor Z-VAD-FMK (Fig. 8b, c).

Coincidently, autophagy is known to be involved in the maintenance of neuronal homeostasis, particularly in response to oxidative stress and mitochondria dysfunction-mediated neurotoxicity [35]. Some reports suggest that autophagy may play a protective role in the process of pro-apoptotic drug-induced apoptosis, such as cisplatin, etoposide, olanzapine, staurosporine, and doxorubicin, contributed to cell survival [27–29, 46]. Several previous studies showed that autophagy can contribute to the alleviation of neuronal apoptosis in rats and can be explained via inhibition of ROS production by autophagy [47–49]. These findings are in-line with our previous study that showed that autophagy may play a protective role in colistin-induced nephrotoxicity [15].

Conclusions

For the first time, our study reveals that colistin-induced neurotoxicity in N2a neuronal cells involves apoptotic pathways associated with the generation of ROS and mitochondrial dysfunction; a putative schematic representation of the potential mechanism is shown in Fig. 9. In response to high colistin exposure, N2a cells appear to activate autophagy salvaging pathways to “mop-up” damaged organelles and proteins. Our findings also touch upon the highly intricate cross talk including ROS, p53, and death receptor pathways. This first-hand understanding of colistin-induced neurotoxicity provides

key information that is important not only for the amelioration of this unwanted side effect but also for the discovery of novel, safer polymyxin-lipopeptide antibiotics, i.e., new "magic bullets" in the battle against MDR gram-negative "superbugs."

Acknowledgments This study was supported by the National Natural Science Foundation of China (award number 31372486). T. V. is supported by a research grant from the National Institute of Allergy and Infectious Diseases of the National Institutes of Health (R01 AI111965). T. V. is also supported by the Australian National Health and Medical Research Council (NHMRC). This study was supported by Chinese Universities Scientific Fund (Award number 2015DY003).

Conflict of interest The authors declare that there are no conflicts of interest.

References

1. Nation RL, Li J, Cars O, Couet W, Dudley MN, Kaye KS, Mouton JW, Paterson DL et al (2014) Framework for optimisation of the clinical use of colistin and polymyxin B: the Prato polymyxin consensus. Lancet Infect Dis. doi:10.1016/S1473-3099(14)70850-3
2. Li J, Nation RL, Turnidge JD, Milne RW, Coulthard K, Rayner CR, Paterson DL (2006) Colistin: the re-emerging antibiotic for multidrug-resistant gram-negative bacterial infections. Lancet Infect Dis 6(9):589–601. doi:10.1016/S1473-3099(06)70580-1
3. Li J, Nation RL, Milne RW, Turnidge JD, Coulthard K (2005) Evaluation of colistin as an agent against multi-resistant Gram-negative bacteria. Int J Antimicrob Agents 25(1):11–25. doi:10.1016/j.ijantimicag.2004.10.001
4. Bergen PJ, Li J, Rayner CR, Nation RL (2006) Colistin methanesulfonate is an inactive prodrug of colistin against Pseudomonas aeruginosa. Antimicrob Agents Chemother 50(6):1953–1958. doi:10.1128/AAC.00035-06
5. Garonzik SM, Li J, Thamlikitkul V, Paterson DL, Shoham S, Jacob J, Silveira FP, Forrest A et al (2011) Population pharmacokinetics of colistin methanesulfonate and formed colistin in critically ill patients from a multicenter study provide dosing suggestions for various categories of patients. Antimicrob Agents Chemother 55(7):3284–3294. doi:10.1128/AAC.01733-10
6. Wahby K, Chopra T, Chandrasekar P (2010) Intravenous and inhalational colistin-induced respiratory failure. Clin Infect Dis 50(6):e38–e40. doi:10.1086/650582
7. Falagas ME, Kasiakou SK (2006) Toxicity of polymyxins: a systematic review of the evidence from old and recent studies. Crit Care 10(1):R27. doi:10.1186/cc3995
8. Honore PM, Jacobs R, Lochy S, De Waele E, Van Gorp V, De Regt J, Martens G, Joannes-Boyau O et al (2013) Acute respiratory muscle weakness and apnea in a critically ill patient induced by colistin neurotoxicity: key potential role of hemoadsorption elimination during continuous venovenous hemofiltration. Int J Nephrol Renovasc Dis 6:107–111. doi:10.2147/IJNRD.S42791
9. Weinstein L, Doan TL, Smith MA (2009) Neurotoxicity in patients treated with intravenous polymyxin B: two case reports. Am J Health Syst Pharm 66(4):345–347. doi:10.2146/ajhp080065
10. Liu Y, Dai C, Gao R, Li J (2013) Ascorbic acid protects against colistin sulfate-induced neurotoxicity in PC12 cells. Toxicol Mech Methods 23(8):584–590. doi:10.3109/15376516.2013.807532
11. Zhang C, Wang C, Tang S, Sun Y, Zhao D, Zhang S, Deng S, Zhou Y et al (2013) TNFR1/TNF-alpha and mitochondria interrelated signaling pathway mediates quinocetone-induced apoptosis in HepG2 cells. Food Chem Toxicol 62:825–838. doi:10.1016/j.fct.2013.10.022
12. Biederbick A, Kern HF, Elsasser HP (1995) Monodansylcadaverine (MDC) is a specific in vivo marker for autophagic vacuoles. Eur J Cell Biol 66(1):3–14
13. Kantara C, O'Connell M, Sarkar S, Moya S, Ullrich R, Singh P (2014) Curcumin promotes autophagic survival of a subset of colon cancer stem cells, which are ablated by DCLK1-siRNA. Cancer Res 74(9):2487–2498. doi:10.1158/0008-5472.CAN-13-3536
14. Shailasree S, Venkataramana M, Niranjana SR, Prakash HS (2015) Cytotoxic effect of p-coumaric acid on neuroblastoma, N2a cell via generation of reactive oxygen species leading to dysfunction of mitochondria inducing apoptosis and autophagy. Mol Neurobiol 51(1):119–130. doi:10.1007/s12035-014-8700-2
15. Dai C, Li J, Tang S, Li J, Xiao X (2014) Colistin-induced nephrotoxicity in mice involves the mitochondrial, death receptor, and endoplasmic reticulum pathways. Antimicrob Agents Chemother 58(7):4075–4085. doi:10.1128/AAC.00070-14
16. Koch-Weser J, Sidel VW, Federman EB, Kanarek P, Finer DC, Eaton AE (1970) Adverse effects of sodium colistimethate. Manifestations and specific reaction rates during 317 courses of therapy. Ann Intern Med 72(6):857–868
17. Dai C, Tang S, Li J, Wang J, Xiao X (2014) Effects of colistin on the sensory nerve conduction velocity and F-wave in mice. Basic Clin Pharmacol Toxicol 115(6):577–580. doi:10.1111/bcpt.12272
18. Bosso JA, Liptak CA, Seilheimer DK, Harrison GM (1991) Toxicity of colistin in cystic fibrosis patients. DICP 25(11):1168–1170
19. Dai C, Li J, Li J (2013) New insight in colistin induced neurotoxicity with the mitochondrial dysfunction in mice central nervous tissues. Exp Toxicol Pathol 65(6):941–948. doi:10.1016/j.etp.2013.01.008
20. Dai C, Li J, Lin W, Li G, Sun M, Wang F, Li J (2012) Electrophysiology and ultrastructural changes in mouse sciatic nerve associated with colistin sulfate exposure. Toxicol Mech Methods 22(8):592–596. doi:10.3109/15376516.2012.704956
21. Wallace SJ, Li J, Nation RL, Rayner CR, Taylor D, Middleton D, Milne RW, Coulthard K et al (2008) Subacute toxicity of colistin methanesulfonate in rats: comparison of various intravenous dosage regimens. Antimicrob Agents Chemother 52(3):1159–1161. doi:10.1128/AAC.01101-07
22. Lin B, Zhang C, Xiao X (2005) Toxicity, bioavailability and pharmacokinetics of a newly formulated colistin sulfate solution. J Vet Pharmacol Ther 28(4):349–354. doi:10.1111/j.1365-2885.2005.00666.x
23. Landman WJ, Dwars RM, Keukens HJ, Berendsen BJ (2000) Polymyxin E-1 (colistin sulphate) (neuro-)intoxication in young ostriches (Struthio camelus spp.). Avian Pathol 29(6):593–601. doi:10.1080/03079450020016841
24. Dai C, Zhang D, Li J (2013) Effect of colistin exposure on calcium homeostasis and mitochondria functions in chick cortex neurons. Toxicol Mech Methods 23(4):281–288. doi:10.3109/15376516.2012.754533
25. Dai C, Zhang D, Gao R, Zhang X, Li J (2013) In vitro toxicity of colistin on primary chick cortex neurons and its potential mechanism. Environ Toxicol Pharmacol 36(2):659–666. doi:10.1016/j.etap.2013.06.013
26. Fu XY, Yang MF, Cao MZ, Li DW, Yang XY, Sun JY, Zhang ZY, Mao LL et al (2014) Strategy to suppress oxidative damage-induced neurotoxicity in PC12 cells by curcumin: the role of ROS-mediated DNA damage and the MAPK and AKT pathways. Mol Neurobiol. doi:10.1007/s12035-014-9021-1
27. Xie BS, Zhao HC, Yao SK, Zhuo DX, Jin B, Lv DC, Wu CL, Ma DL et al (2011) Autophagy inhibition enhances etoposide-induced cell death in human hepatoma G2 cells. Int J Mol Med 27(4):599–606. doi:10.3892/ijmm.2011.607

28. Ha JY, Kim JS, Kim SE, Son JH (2014) Simultaneous activation of mitophagy and autophagy by staurosporine protects against dopaminergic neuronal cell death. Neurosci Lett 561:101–106. doi:10.1016/j.neulet.2013.12.064
29. Fulda S, Debatin KM (2006) Extrinsic versus intrinsic apoptosis pathways in anticancer chemotherapy. Oncogene 25(34):4798–4811. doi:10.1038/sj.onc.1209608
30. Tait SW, Green DR (2010) Mitochondria and cell death: outer membrane permeabilization and beyond. Nat Rev Mol Cell Biol 11(9):621–632. doi:10.1038/nrm2952
31. Rasola A, Bernardi P (2007) The mitochondrial permeability transition pore and its involvement in cell death and in disease pathogenesis. Apoptosis 12(5):815–833. doi:10.1007/s10495-007-0723-y
32. Li PF, Dietz R, von Harsdorf R (1999) p53 regulates mitochondrial membrane potential through reactive oxygen species and induces cytochrome c-independent apoptosis blocked by Bcl-2. EMBO J 18(21):6027–6036. doi:10.1093/emboj/18.21.6027
33. Yuan L, Wei S, Wang J, Liu X (2014) Isoorientin induces apoptosis and autophagy simultaneously by reactive oxygen species (ROS)-related p53, PI3K/Akt, JNK, and p38 signaling pathways in HepG2 cancer cells. J Agric Food Chem 62(23):5390–5400. doi:10.1021/jf500903g
34. Ehrhardt H, Hacker S, Wittmann S, Maurer M, Borkhardt A, Toloczko A et al (2008) Cytotoxic drug-induced, p53-mediated upregulation of caspase-8 in tumor cells. Oncogene 27(6):783–793. doi:10.1038/sj.onc.1210666
35. Wu HJ, Pu JL, Krafft PR, Zhang JM, Chen S (2015) The molecular mechanisms between autophagy and apoptosis: potential role in central nervous system disorders. Cell Mol Neurobiol 35(1):85–99. doi:10.1007/s10571-014-0116-z
36. Ikonomidou C, Kaindl AM (2011) Neuronal death and oxidative stress in the developing brain. Antioxid Redox Signal 14(8):1535–1550. doi:10.1089/ars.2010.3581
37. Lee J, Giordano S, Zhang J (2012) Autophagy, mitochondria and oxidative stress: cross-talk and redox signalling. Biochem J 441(2):523–540. doi:10.1042/BJ20111451
38. Stowe DF, Camara AK (2009) Mitochondrial reactive oxygen species production in excitable cells: modulators of mitochondrial and cell function. Antioxid Redox Signal 11(6):1373–1414. doi:10.1089/ARS.2008.2331
39. Dai C, Tang S, Deng S, Zhang S, Zhou Y, Velkov T, Li J, Xiao X (2015) Lycopene attenuates colistin-induced nephrotoxicity in mice via activation of the Nrf2/HO-1 pathway. Antimicrob Agents Chemother 59(1):579–585. doi:10.1128/AAC.03925-14
40. Marino G, Niso-Santano M, Baehrecke EH, Kroemer G (2014) Self-consumption: the interplay of autophagy and apoptosis. Nat Rev Mol Cell Biol 15(2):81–94. doi:10.1038/nrm3735
41. Verschooten L, Barrette K, Van Kelst S, Rubio Romero N, Proby C, De Vos R, Agostinis P, Garmyn M (2012) Autophagy inhibitor chloroquine enhanced the cell death inducing effect of the flavonoid luteolin in metastatic squamous cell carcinoma cells. PLoS One 7(10):e48264. doi:10.1371/journal.pone.0048264
42. Guo XL, Li D, Hu F, Song JR, Zhang SS, Deng WJ, Sun K, Zhao QD et al (2012) Targeting autophagy potentiates chemotherapy-induced apoptosis and proliferation inhibition in hepatocarcinoma cells. Cancer Lett 320(2):171–179. doi:10.1016/j.canlet.2012.03.002
43. Li J, Hou N, Faried A, Tsutsumi S, Takeuchi T, Kuwano H (2009) Inhibition of autophagy by 3-MA enhances the effect of 5-FU-induced apoptosis in colon cancer cells. Ann Surg Oncol 16(3):761–771. doi:10.1245/s10434-008-0260-0
44. Xiong HY, Guo XL, Bu XX, Zhang SS, Ma NN, Song JR, Hu F, Tao SF et al (2010) Autophagic cell death induced by 5-FU in Bax or PUMA deficient human colon cancer cell. Cancer Lett 288(1):68–74. doi:10.1016/j.canlet.2009.06.039
45. Wu H, Che X, Zheng Q, Wu A, Pan K, Shao A, Wu Q, Zhang J et al (2014) Caspases: a molecular switch node in the crosstalk between autophagy and apoptosis. Int J Biol Sci 10(9):1072–1083. doi:10.7150/ijbs.9719
46. Altman BJ, Rathmell JC (2009) Autophagy: not good OR bad, but good AND bad. Autophagy 5(4):569–570
47. Shao A, Wang Z, Wu H, Dong X, Li Y, Tu S, Tang J, Zhao M et al (2014) Enhancement of autophagy by histone deacetylase inhibitor trichostatin a ameliorates neuronal apoptosis after subarachnoid hemorrhage in rats. Mol Neurobiol. doi:10.1007/s12035-014-8986-0
48. Wang H, Gao N, Li Z, Yang Z, Zhang T (2015) Autophagy alleviates melamine-induced cell death in PC12 cells via decreasing ROS level. Mol Neurobiol. doi:10.1007/s12035-014-9073-2
49. Tang P, Hou H, Zhang L, Lan X, Mao Z, Liu D, He C, Du H et al (2014) Autophagy reduces neuronal damage and promotes locomotor recovery via inhibition of apoptosis after spinal cord injury in rats. Mol Neurobiol 49(1):276–287. doi:10.1007/s12035-013-8518-3